

Nonequilibrium Theory of Photoinduced Valley Hall Effect

I. Vakulchyk,^{1,2} V. M. Kovalev,^{3,4} and I. G. Savenko^{1,2}

¹*Center for Theoretical Physics of Complex Systems,
Institute for Basic Science (IBS), Daejeon 34126, Korea*

²*Basic Science Program, Korea University of Science and Technology (UST), Daejeon 34113, Korea*

³*Rzhanov Institute of Semiconductor Physics, Siberian Branch of Russian Academy of Sciences, Novosibirsk 630090, Russia*

⁴*Novosibirsk State Technical University, Novosibirsk 630073, Russia*

(Dated: May 2, 2022)

A recent scientific debate has arisen: Which processes underlie the actual ground of the valley Hall effect (VHE) in two-dimensional materials? The original VHE emerges in samples with ballistic transport of electrons due to the anomalous velocity terms resulting from the Berry phase effect. In disordered samples though, alternative mechanisms associated with electron scattering off impurities have been suggested: (i) asymmetric electron scattering, called skew-scattering, and (ii) a shift of the electron wave packet in real space, called a side-jump. It has been claimed that the side-jump not only contributes to the VHE but fully offsets the anomalous terms regardless of the drag force for fundamental reasons, and thus, the side-jump together with skew scattering become the dominant mechanisms. However, this claim is based on equilibrium theories without any external valley-selective optical pumping, which makes the results fundamentally interesting but incomplete and impracticable. We develop in this work the first microscopic theory of the photoinduced VHE using the Keldysh nonequilibrium diagrammatic technique, and find out that the asymmetric skew scattering mechanism is dominant in the vicinity of the interband absorption edge.

Introduction.— The concept of the Hall effect is the emergence of an electric current or other flux of particles in a sample in the direction transverse to both the dragging force and the external magnetic field, which should be finite in order for the effect to take place. If similar phenomena happen in the absence of a magnetic field, they are referred to as *anomalous Hall effects* (AHEs) [1]. The eminent examples of the AHE include the Hall effect in magnetic materials (with their built-in sample magnetization), the spin Hall effect, where the role of the magnetic field is played by spin-orbit interaction, and the valley Hall effect (VHE) [2–5], which emerges in two-dimensional (2D) Dirac materials possessing nonequivalent valleys in reciprocal space, like transition metal dichalcogenide (TMDC) monolayers [6–8]. There, electrons and holes occupy two valleys, K and K', that are connected by time-reversal symmetry. TMDCs also represent a promising platform and testing ground for optoelectronics [9, 10] and spin-valleytronics [11] as direct-bandgap materials that obey valley-dependent optical selection rules [12, 13]. These properties make them fundamentally interesting and appealing for device design [14].

It is commonly accepted that there exist three principal mechanisms behind the AHE in non-magnetic materials [15]: (i) the Berry phase stipulated anomalous velocity term (also called the intrinsic contribution) [16], (ii) the side-jump contribution, and (iii) the skew scattering (asymmetric) contribution. These three terms interplay and can partially compensate each other, as has been reported in recent works on electron [17, 18] and exciton [19] transport in semiconductors. In particular, one recent important work [18] shows that the side-jump and skew scattering should not be disregarded under photon or phonon drag conditions, as it is usually done when

considering the VHE [2, 4, 16, 20]. More precisely, it has been demonstrated that the side-jump compensates for the intrinsic contribution to conductivity, and moreover, some terms in the side-jump survive.

These fundamental conclusions undoubtedly play an important role in our understanding of the microscopic processes underlying the VHE. However, the existing theories only consider equilibrium electrons initially occupying two nonequivalent valleys. The valley Hall currents resulting from these electrons flow in opposite directions, and being of the same magnitude the currents cancel each other out, leaving zero-net VHE current in the sample. To observe a nonzero valley Hall current in actual experiments [3], the sample should be illuminated by an external circularly polarized electromagnetic field of light. This destroys the time-reversal symmetry and predominantly populates only one of the valleys due to the valley-dependent interband optical selection rules. As a result, the current contributions from nonequivalent valleys do not annul each other. It is important, then, to consider nonequilibrium photo-excited electrons since they are the ones actually contributing to the VHE. While this idea has been briefly mentioned in literature [21], it has not been rigorously studied. In the meantime though, the light-induced AHE has generally become an active field of research [22]. Analysis [3] of experimental VHE observations is based on a phenomenological expression of the form $\sigma_H \propto \delta n$, where σ_H is the valley Hall conductivity and δn is the electron density imbalance between the valleys due to interband photogeneration. The standard derivation of this dependence is based on the Berry-phase-related expression applicable to ballistic samples.

In this Letter, we analyze the applicability of this approach in the presence of all relevant electron-impurity

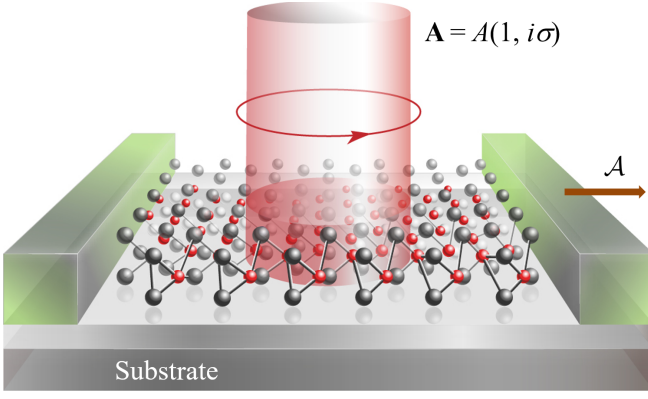


FIG. 1. System schematic of a 2D Dirac material exposed to circularly polarized light \mathbf{A} and static drag field \mathcal{A} . The light couples to the K or K' valley depending on its polarization σ .

scattering processes. We pose an intriguing question: Do these statements (regarding the partial compensation of the intrinsic contribution) remain valid in the case of optically driven systems based on Dirac materials when circularly polarized light pumps one of the valleys? The answer to this question is of utmost importance not only from a fundamental viewpoint (since 2D Dirac materials are prone to interact with light) but also from the perspective of optoelectronic applications, in particular, in novel van der Waals heterostructures. We consider the intrinsic, side-jump, and skew scattering contributions to valley Hall photoconductivity using the nonequilibrium Keldysh diagram technique. Thus, we build a microscopic theory of the photoinduced VHE. To investigate the transport properties of nonequilibrium photo-excited electrons and their role in VHE, we will assume that the valence band (v-band) is fully filled and the conduction band (c-band) is nearly empty, and thus only the photo-excited electrons contribute to the VHE while the possible presence of equilibrium electrons in the valleys does not obscure the phenomena under study.

General theory.— We consider a 2D system (Fig. 1) exposed to a circularly polarized light (which results in interband transitions),

$$\mathbf{A}(t) = \mathbf{A}e^{-i\omega t} + \mathbf{A}^*e^{i\omega t}, \quad (1)$$

and thus $\mathbf{A} = A(1, i\sigma)$ with $\sigma = \pm 1$, and the in-plane alternating drag electric field is

$$\mathcal{A}(t) = \mathcal{A}(e^{-i\Omega t} + e^{i\Omega t}), \quad (2)$$

where we assume that the drag field is linearly polarized so \mathcal{A} is real-valued. At the end of the calculations, we will put $\Omega \rightarrow 0$ to find the static limit, which corresponds to the drag effect. We define the coordinates such that the drag field is directed along the y axis, and therefore our goal is to consider the valley Hall current along x .

The full system Hamiltonian reads ($e < 0$)

$$H = \frac{\Delta}{2} \hat{s}_z + \mathbf{V} \cdot \mathbf{p} - e\mathbf{V} \cdot \mathbf{A}(t) - eV^y \mathcal{A}(t), \quad (3)$$

where Δ is the monolayer material bandgap, $\mathbf{p} = p(\cos \phi, \sin \phi)$ is the electron momentum, $\mathbf{V} = v_0(\eta \hat{s}_x, \hat{s}_y)$ is the velocity, $\eta = \pm 1$ is the valley index, and \hat{s}_α are the Pauli matrices with $\alpha = x, y, z$. The Hamiltonian (3) is written in sub-lattice basis since the honeycomb lattice of a TMDC monolayer can be looked at as two triangle sub-lattices inserted into each other. However, it is instructive and physically transparent to work in the c- and v-band basis (the *cv-basis* in what follows). In our case, the external fields in (3) are uniform in space, thus conserving the electron momentum (which, hence, can be considered as a c-number). To transform into the cv-basis, we use a unitary operator that depends only on the electron momentum [23],

$$U = \begin{pmatrix} \cos(\theta/2) & \sin(\theta/2) \\ \sin(\theta/2)e^{i\eta\phi} & -\cos(\theta/2)e^{i\eta\phi} \end{pmatrix}, \quad (4)$$

where $\cos \theta = \Delta/2\epsilon_p$, $\sin \theta = \eta v_0 p/\epsilon_p$, and $\epsilon_p = \sqrt{(\Delta/2)^2 + v_0^2 p^2} \approx \Delta/2 + p^2/2m$, where the electron effective mass is $m = \Delta/(2v_0^2)$ at small electron momenta, $v_0 p \ll \Delta$. Using $\mathcal{H} = U^\dagger H U$, we find

$$\mathcal{H} = \mathcal{H}_0 - e\mathbf{v} \cdot \mathbf{A}(t) - ev^y \mathcal{A}(t), \quad (5)$$

where

$$\mathcal{H}_0 = \begin{pmatrix} \epsilon_c(p) & 0 \\ 0 & \epsilon_v(p) \end{pmatrix}, \quad \mathbf{v} = \begin{pmatrix} \mathbf{v}_{cc} & \mathbf{v}_{cv} \\ \mathbf{v}_{vc} & \mathbf{v}_{vv} \end{pmatrix} \quad (6)$$

are the bare Hamiltonian and the velocity operator in the cv-basis, with $\epsilon_c(p) \equiv \epsilon_p$ and $\epsilon_v(p) = -\epsilon_p$ (we will just write ϵ_c and ϵ_v in what follows, keeping in mind that they both depend on the absolute value of the momentum; we will also omit \hbar in the expressions below but restore it in the final formulas).

The valley Hall current, being the linear response to external drag field \mathcal{A} , reads [24],

$$j_x(t) = \int_{\mathcal{C}} dt' Q_{xy}(t, t') \mathcal{A}(t'), \quad (7)$$

$$Q_{xy}(t, t') = ie^2 \text{Tr} [v^x G(t, t') v^y G(t', t)], \quad (8)$$

where \mathcal{C} stands for the Keldysh contour, Tr is the trace operator that should be taken over the bands, and

$$[i\partial_t - \mathcal{H}_0 + e\mathbf{v} \cdot \mathbf{A}(t)] G(t, t') = \delta(t - t') \quad (9)$$

defines the matrix Green's function in the cv-basis. It should be stressed that this (matrix) Green's function accounts exactly for the external pumping field. We can also write (7) as

$$j_x(t) = j_x^{(1)}(\Omega) e^{-i\Omega t} + j_x^{(1)}(-\Omega) e^{i\Omega t}. \quad (10)$$

The in-plane electric field is $E_y(t) = -\partial_t \mathcal{A}(t)$, and the current can be found as $j_x(\Omega) = \mathcal{A}[Q_{xy}(\Omega, \omega) + Q_{xy}(-\Omega, \omega)]$. Also, we define $j_x(\omega) = \sigma_H(\omega)E_y$. It is then possible to express the static (with respect to in-plane electric field E_y) valley Hall photoconductivity by the standard formula [24],

$$\sigma_H(\omega) = \lim_{\Omega \rightarrow 0} \frac{Q_{xy}(\Omega, \omega) - Q_{xy}(-\Omega, \omega)}{2i\Omega}. \quad (11)$$

To find this, we have to consider the Green's function of the electrons in the c-band while accounting for interband pumping. This Green's function, G , being the solution of (9), represents a matrix defined on the Keldysh contour, with the retarded (advanced) component $G^{R(A)}$ and the lesser component $G^<(\varepsilon) = f_0(\varepsilon)[G^A(\varepsilon) - G^R(\varepsilon)]$, where $f_0(\varepsilon)$ is the stationary nonequilibrium distribution function of the c-band electrons under interband pumping. This stationary nonequilibrium electron distribution is characterized by the balance of electron generation and recombination. Thus, the retarded and advanced Green's functions read $G^{R,A} = (\varepsilon - \varepsilon_c \pm i/2\tau_i \pm i/2\tau_r)^{-1}$, where τ_i is the (intraband) electron momentum scattering time over impurities, and τ_r is the interband recombination time, or in other words, the lifetime of the electrons in the c-band.

The nonequilibrium distribution function can be directly found from the equation of balance expressing the equality of generation and recombination processes in the form $f_0(\varepsilon)/\tau_r = g(\varepsilon)$, where the generation probability is $g(\varepsilon) = 2\pi|M_{cv}(\mathbf{p}=0)|^2\delta(\varepsilon - \omega - \varepsilon_v)$. Here, the interband matrix element, $|M_{cv}(0)|^2 = |\mathbf{e}\mathbf{v}_{cv}\mathbf{A}|^2 = e^2v_0^2A^2(\eta + \sigma)^2$, is taken in the vicinity of the bottom of the c-band, $\mathbf{p} \approx 0$. This regime is the most interesting for us since electrons find themselves in the c-band from optical absorption or scattering by impurities only, and thus we can disregard other sources of conducting electrons (such as the thermal ionization of shallow impurities). Then, the (vertical) optical transitions occur at very small electron momenta p . The factor $(\eta + \sigma)^2$ reflects the valley-selective interband optical rules for the circularly polarized pumping electromagnetic field. Finally, for the distribution function we find $f_0(\varepsilon) = 2\pi\tau_r|M_{cv}(0)|^2\delta(\varepsilon - \omega - \varepsilon_v)$. The same expression can be found by the Feynman diagrams technique [25]. Indeed, the bare self-energy of the photo-excited electrons in the c-band reads $\Sigma_c^<(\varepsilon) = |M_{cv}(0)|^2G_v(\varepsilon - \omega)$, as seen Fig. 2(a). The ladder renormalization of this expression [Fig. 2(b)] gives the lesser Green's function $G_c^<(\varepsilon) = 2\pi i f_0(\varepsilon)\delta(\varepsilon - \varepsilon_c)$, where the distribution function $f(\varepsilon)$ has the same form as the one found from the equation of balance discussed above. Having defined the Green's functions describing the stationary nonequilibrium state, we can now analyze all the contributions to the photoinduced VHE.

Intrinsic contribution.— The intrinsic contribution is associated with the Berry phase of the electrons in a given valley. It constitutes several diagrams of the kind

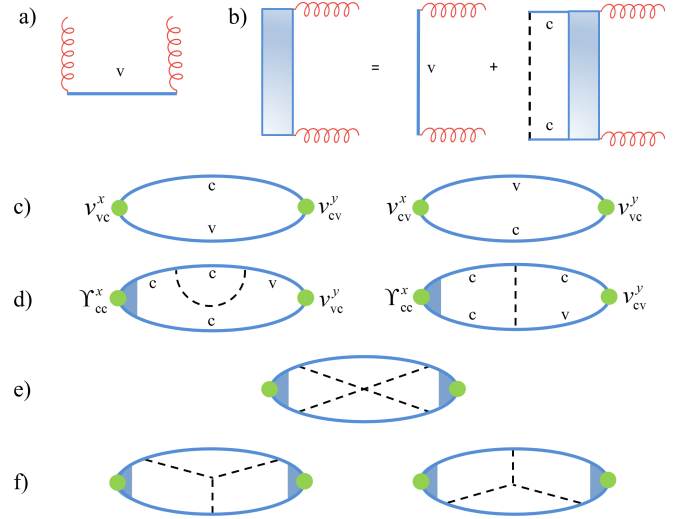


FIG. 2. Feynman diagrams for the photoinduced VHE. a) Bare self-energy of the photoinduced electrons in the conduction band. b) Integral equation for the renormalized self-energy. c) The intrinsic contribution. d) Examples of side-jump diagrams. e) The X-diagram (coherent skew scattering) contribution. f) Anisotropic skew-scattering diagrams. The red helices stand for the external circularly polarized light $\mathbf{A}(t)$; v^x and v^y are the velocity vertices, c and v respectively mark the Green's functions of the electrons in the conduction and valence bands, and the dotted lines indicate impurity scattering.

depicted in Fig. 2(c). Each of these diagrams contains the interband matrix elements of velocity vertices v^x and v^y . In our case, when the Fermi level is in the material bandgap, the contribution of these diagrams consists of two terms having a different physical meaning. The first one is also present in the equilibrium state, and it is associated with the occupied v-band possessing a topological nature. The second contribution is directly associated with the nonequilibrium state and is determined by the photo-excited electrons in the c-band and holes in the v-band. Within the simple symmetric two-band model of Dirac bands in MoS₂ monolayer, the holes' contribution has the same form and just doubles the result. Calculation of the terms illustrated in Fig. 2(c) gives (restoring \hbar)

$$\sigma_H^{(I)} = 2\eta \frac{e^2}{h} \left(\frac{\hbar v_0}{\Delta} \right)^2 n_e, \quad (12)$$

where $n_e = \sum_{\mathbf{p}} f_0[\varepsilon_c(\mathbf{p})]$ is the density of the photo-excited electrons in the c-band of a given valley. This contribution has the same structure as the one in the equilibrium case; the principal difference is that n_e represents here the density of photo-excited electrons instead of the density of thermally-equilibrium electrons.

Side-jump contribution.— The diagrams representing the side-jump contribution contain the interband matrix element of electron-impurity scattering as it is depicted

in Fig. 2(d). Each of these diagrams has a counterpart (mirror reflections with respect to the vertical and horizontal lines) [25].

In order to calculate the conductivity due to the side-jump impurity process, let us first introduce the impurity potential in the cv-basis in the elastic scattering approximation [17],

$$u(\mathbf{p}, \mathbf{p}') = u^0(\mathbf{p}, \mathbf{p}') \left\{ \left[1 - \sin^2 \left(\frac{\theta}{2} \right) (1 - e^{i\eta(\phi' - \phi)}) \right] \times \frac{\hat{s}_0 + \hat{s}_z}{2} + \left[1 - \cos^2 \left(\frac{\theta}{2} \right) (1 - e^{i\eta(\phi' - \phi)}) \right] \frac{\hat{s}_0 - \hat{s}_z}{2} + \frac{1}{2} \sin \theta (1 - e^{i\eta(\phi' - \phi)}) \hat{s}_x \right\}, \quad (13)$$

where \hat{s}_0 is the unity matrix, ϕ and ϕ' are the angles corresponding to the momenta \mathbf{p} and \mathbf{p}' , respectively, and $\langle |u^0(\mathbf{p}, \mathbf{p}')|^2 \rangle = n_i u_0^2$ with n_i being the density of impurities and $n_i u_0^2 = (m\tau_i)^{-1}$. Here $\langle \dots \rangle$ stands for the averaging over the positions of impurities. Following [17], we should, first, find the renormalized velocity vertex, $\Upsilon_{cc}^\beta(\mathbf{p})$, the integral equation of which reads

$$\Upsilon_{cc}^\beta(\mathbf{p}) = v_{cc}^\beta(\mathbf{p}) + \int \frac{d\mathbf{p}'}{(2\pi)^2} \Upsilon_{cc}^\beta(\mathbf{p}') \overline{|u_{cc}(\mathbf{p}, \mathbf{p}')|^2} G_c^R(\mathbf{p}', \varepsilon) G_c^A(\mathbf{p}', \varepsilon - \Omega), \quad (14)$$

where $\beta = x, y$ and from (13) we find

$$\overline{|u_{cc}(\mathbf{p}, \mathbf{p}')|^2} = n_i u_0^2 \left| 1 - \sin^2 \left(\frac{\theta}{2} \right) (1 - e^{i\eta(\phi' - \phi)}) \right|^2. \quad (15)$$

Since we consider the transitions to the bottom of the c-band, and thus $p \approx 0$, we can safely neglect the terms $\sin^2(\frac{\theta}{2}) \sim p^2$ as compared to 1. In this case, the integral in (14) equals zero, and accordingly $\Upsilon_{cc}^x \approx v_{cc}^x$ with good accuracy, meaning that the vertex does not renormalize in the vicinity of the bottom of the c-band. Thus, the impurity lines only give averages of the kind

$$\overline{u_{cc}(\mathbf{p}, \mathbf{p}') G_\alpha(\mathbf{p}', \delta t) u_{cv}(\mathbf{p}', \mathbf{p})} \approx \frac{1}{m\tau_i} \int \frac{d\mathbf{p}'}{(2\pi\hbar)^2} \left\{ \sin(\theta) \frac{1 - e^{i\eta(\phi - \phi')}}{2} \right\} G_\alpha(\mathbf{p}', \delta t), \quad (16)$$

along with their complex conjugates. Performing the diagram calculations taking into account the mass operator renormalization [see Fig. 2(b)] we find (see Supplemental Material [25])

$$\sigma_H^{(SJ)} = -4\eta \frac{e^2}{\hbar} \left(\frac{\hbar v_0}{\Delta} \right)^2 \frac{n_e}{2\tau_i \gamma}, \quad (17)$$

where $\gamma = (\tau_i + \tau_r)/2\tau_i\tau_r$ includes the recombination time τ_r reflecting the nonequilibrium nature of the effect. Again, the contribution of the side-jump process is determined by the density of the photo-excited electrons, n_e .

Coherent skew scattering.— The skew mechanism is associated with asymmetric electron scattering by impurities. It should be described beyond the standard Born approximation in electron-impurity scattering probability. Coherent skew scattering involves pairs of closely located impurities, and can be illustrated by a diagram with crossed impurity lines [Fig. 2(e)]. In the framework of standard Drude theory, the diagrams possessing crossing impurity lines are parametrically small and usually do not play any role (except for the theory of weak localization, where maximally crossed diagrams are responsible for the effect). Nevertheless, the so-called X - and Ψ -type diagrams play an essential role in the AHE [26, 27]. For a delta-correlated disorder, the contribution of the Ψ -diagram vanishes, leaving only the X -diagram for calculation (see [25]),

$$\sigma_H^{(X)} = 2\eta \frac{e^2}{\hbar} \left(\frac{\hbar v_0}{\Delta} \right)^2 \frac{n_e}{(2\tau_i \gamma)^2}. \quad (18)$$

Summing up Eqs. (12), (17), and (18), we find

$$\begin{aligned} \sigma_H^{(I)} + \sigma_H^{(SJ)} + \sigma_H^{(X)} &= 2\eta \frac{e^2}{\hbar} \left(\frac{\hbar v_0}{\Delta} \right)^2 n_e \left(1 - \frac{1}{2\tau_i \gamma} \right)^2 \\ &= 2\eta \frac{e^2}{\hbar} \left(\frac{\hbar v_0}{\Delta} \right)^2 n_e \left(1 - \frac{\tau_r}{\tau_r + \tau_i} \right)^2. \end{aligned} \quad (19)$$

In the limit $\tau_r \rightarrow \infty$ and assuming n_e to be the equilibrium electron density, we recover the known result of the equilibrium VHE, when these three contributions cancel each other out [18]. The typical values of the times are $\tau_r \sim \mu\text{s}$ and $\tau_i \sim \text{ps}$, i.e. $\tau_r \gg \tau_i$, allowing us to conclude that the mutual impact of these three contributions on the photoinduced VHE is negligibly small.

Asymmetric skew scattering.— The last principal mechanism is associated with asymmetric electron skew scattering by impurities [Fig. 2(e)]. It should also be described beyond the Born approximation [18] and requires a non-vanishing impurity potential correlator of the third order. The corresponding Y -type Feynman diagrams, as in Fig. 2(f), have one-to-one correspondence with the Boltzmann equation result with an account of the asymmetric contribution to the electron-impurity collision integral [17, 18, 28]. The calculation gives

$$\sigma_H^{(Y)} = -\eta \frac{e^2}{\hbar} \left(\frac{u_0 n_e}{\Delta} \right) \frac{\langle \varepsilon \rangle \tau_i}{(2\gamma \tau_i)^2 \hbar}, \quad (20)$$

where $\langle \varepsilon \rangle = n_e^{-1} \sum_{\mathbf{p}} (\varepsilon_p - \Delta/2) f_0[\varepsilon_c(\mathbf{p})] = (\hbar\omega - \Delta)/2$ is the mean energy of the photo-excited electrons in c-band. Evidently, the asymmetric skew scattering gives the dominant contribution to the photoinduced VHE, since the other contributions vanish, as we have shown above.

Discussion.— Let us consider the approximations employed herein. First of all, photoinduced VHE conductivity contains the density of the photo-excited electrons,

$$n_e = \frac{m\tau_r |M_{cv}(0)|^2}{2\hbar^3} \theta[\omega - \Delta], \quad (21)$$

which has been derived by treating the external circularly polarized pump field as a perturbation. This is only valid as long as $\tau_r|M_{cv}(0)|/\hbar \ll 1$. In the opposite regime, $\tau_r|M_{cv}(0)|/\hbar \gg 1$, the pumping field cannot be considered as a perturbation. While a full theory of the photoinduced VHE in the strong-coupling regime is still missing, the intrinsic contribution (which dominates in ballistic samples) has been studied [23].

The second limitation concerns the electron-impurity scattering: \hbar/τ_i should be small in comparison with the mean value of electron energy. In the case of the stationary nonequilibrium VHE, the characteristic energy of the photo-excited electrons is $\langle \epsilon \rangle$, and thus $(\hbar\omega - \Delta)\tau_i/\hbar \gg 1$ should be fulfilled.

Furthermore, we have accounted for one principle mechanism resulting in the establishment of a stationary nonequilibrium state of photo-excited electrons: the interband recombination. In principle, there also exist other mechanisms limiting electron lifetime in the band. Among them is intervalley electron scattering via impurities or phonons, where such transitions require large values of electron momentum transfer resulting in long electron lifetimes (comparable with τ_r). Another mechanism is electron capture by impurities. These phenomena may play an important role in the photoinduced VHE and require a separate consideration.

In conclusion, we have developed a microscopic theory of the photoinduced valley Hall effect in two-dimensional Dirac materials employing the Keldysh nonequilibrium diagrammatic technique and analyzing the impurity scattering mechanisms under the nonequilibrium conditions. We have demonstrated that while in ballistic samples the intrinsic Berry-phase related term is dominating, in disordered samples the main contribution to the Hall photoconductivity stems from asymmetric skew scattering, with the other principal contributions canceling each other out.

We thank M. Glazov, L. Golub, and A. Parafilo for useful discussions and important advice, J. Rasmussen (RECON) for a critical reading of our manuscript, and E. Savenko for help with the figures. We have been supported by the Institute for Basic Science in Korea (Project No. IBS-R024-D1) and the Russian Science Foundation (Project No. 17-12-01039).

-
- [1] N. Nagaosa, J. Sinova, S. Onoda, A. H. MacDonald, and N. P. Ong, *Rev. Mod. Phys.* **82**, 1539 (2010).
 [2] D. Xiao, G.-B. Liu, W. Feng, X. Xu, and W. Yao, *Phys.*

- Rev. Lett.* **108**, 196802 (2012).
 [3] K. F. Mak, K. L. McGill, J. Park, and P. L. McEuen, *Science* **344**, 1489 (2014).
 [4] A. V. Kalameitsev, V. M. Kovalev, and I. G. Savenko, *Phys. Rev. Lett.* **122**, 256801 (2019).
 [5] C. Jin, J. Kim, M. I. B. Utama, E. C. Regan, H. Kleeemann, H. Cai, Y. Shen, M. J. Shinner, A. Sengupta, K. Watanabe, T. Taniguchi, S. Tongay, A. Zettl, and F. Wang, *Science* **360**, 893 (2018).
 [6] X. Xu, W. Yao, D. Xiao, and T. F. Heinz, *Nature Phys.* **10**, 343 (2014).
 [7] N. Ubrig, S. Jo, M. Philippi, D. Costanzo, H. Berger, A. B. Kuzmenko, and A. F. Morpurgo, *Nano Letters* **17**, 5719 (2017).
 [8] Y. Liu, Y. Gao, S. Zhang, J. He, J. Yu, and Z. Liu, *Nano Res.* **12**, 2695 (2019).
 [9] J. Sun, H. Hu, D. Pan, S. Zhang, and H. Xu, *Nano Letters* **20**, 4953 (2020).
 [10] S. Kang, D. Lee, J. Kim, A. Capasso, H. S. Kang, J.-W. Park, C.-H. Lee, and G.-H. Lee, *2D Mater.* **7**, 022003 (2020).
 [11] Y. Ominato, J. Fujimoto, and M. Matsuo, *Phys. Rev. Lett.* **124**, 166803 (2020).
 [12] D. Xiao, W. Yao, and Q. Niu, *Phys. Rev. Lett.* **99**, 236809 (2007).
 [13] W. Yao, D. Xiao, and Q. Niu, *Phys. Rev. B* **77**, 235406 (2008).
 [14] L. Li, L. Shao, X. Liu, A. Gao, H. Wang, B. Zheng, G. Hou, K. Shehzad, L. Yu, F. Miao, Y. Shi, Y. Xu, and X. Wang, *Nature Nanotechnol.* (2020), 10.1038/s41565-020-0727-0.
 [15] M. I. Dyakonov, *Spin physics in semiconductors*, 2nd ed., Vol. 157 (Springer, Berlin, Heidelberg, 2017).
 [16] D. Xiao, M.-C. Chang, and Q. Niu, *Rev. Mod. Phys.* **82**, 1959 (2010).
 [17] N. A. Sinitsyn, A. H. MacDonald, T. Jungwirth, V. K. Dugaev, and J. Sinova, *Phys. Rev. B* **75**, 045315 (2007).
 [18] M. M. Glazov and L. E. Golub, *Phys. Rev. B* **102**, 155302 (2020).
 [19] M. M. Glazov and L. E. Golub, *Phys. Rev. Lett.* **125**, 157403 (2020).
 [20] M. Onga, Y. Zhang, T. Ideue, and Y. Iwasa, *Nature Mat.* **16**, 1193 (2017).
 [21] T. Olsen and I. Souza, *Phys. Rev. B* **92**, 125146 (2015).
 [22] J. W. McIver, B. Schulte, F.-U. Stein, T. Matsuyama, G. Jotzu, G. Meier, and A. Cavalleri, *Nature Phys.* **16**, 38–41 (2020).
 [23] V. M. Kovalev, W.-K. Tse, M. V. Fistul, and I. G. Savenko, *New J. Phys.* **20**, 083007 (2018).
 [24] G. D. Mahan, *Many-Particle Physics* (Plenum Press, New York and London, 1990).
 [25] See Supplemental Material at [URL], which gives the details of the derivations of the main formulas.
 [26] I. A. Ado, I. A. Dmitriev, P. M. Ostrovsky, and M. Titov, *Europhys. Lett.* **111**, 37004 (2015).
 [27] I. A. Ado, I. A. Dmitriev, P. M. Ostrovsky, and M. Titov, *Phys. Rev. B* **96**, 235148 (2017).
 [28] N. A. Sinitsyn, *J. Phys: Cond. Matt.* **20**, 023201 (2007).